Food and Chemical Toxicology 130 (2019) 219–230

Contents lists available at ScienceDirect

Food and Chemical Toxicology

journal homepage: www.elsevier.com/locate/foodchemtox

Pseudomonas aeruginosa-derived pyocyanin reduces adipocyte differentiation, body weight, and fat mass as mechanisms contributing to septic cachexia

Nika Larian[a], Mark Ensor[a], Sean E. Thatcher[a], Victoria English[a], Andrew J. Morris[b], Arnold Stromberg[c], Lisa A. Cassis[a,*]

[a] Department of Pharmacology and Nutritional Sciences, University of Kentucky, Lexington, KY, USA
[b] Department of Internal Medicine,University of Kentucky, Lexington, KY, USA
[c] Department of Statistics, University of Kentucky, Lexington, KY, USA

ARTICLE INFO

Keywords:
Pyocyanin
Pseudomonas aeruginosa
Adipocyte
Sepsis
Cachexia
Aryl hydrocarbon receptor

ABSTRACT

Pseudomonas aeruginosa, a leading cause of sepsis, produces pyocyanin, a blue-pigmented virulence factor. Sepsis is associated with cachexia, but mechanisms are unknown and conventional nutrition approaches are not effective treatments. Pyocyanin has affinity for the aryl hydrocarbon receptor (AhR), which is expressed on adipocytes and regulates adipocyte differentiation. The purpose of this study was to define *in vitro* and *in vivo* effects of pyocyanin on adipocyte differentiation and body weight regulation as relates to septic cachexia. In 3T3-L1 preadipocytes, pyocyanin activated AhR and its downstream marker CYP1a1, and reduced differentiation. Administration of pyocyanin to male C57BL/6J mice acutely reduced body temperature with altered locomotion, but caused sustained weight loss. Chronic pyocyanin administration to male and female C57BL/6J mice resulted in sustained reductions in body weight and fat mass, with adipose-specific AhR activation. Pyocyanin-treated male mice had decreased energy expenditure and physical activity, and increased adipose explant lipolysis. In females, pyocyanin caused robust reductions in body weight, adipose-specific AhR activation, and increased expression of inflammatory cytokines in differentiated adipocytes. These results demonstrate that pyocyanin reduces adipocyte differentiation and decreases body weight and fat mass in male and female mice, suggesting that pyocyanin may play a role in septic cachexia.

1. Introduction

Sepsis is a life-threatening condition characterized by dysregulated host response to infection and multiple organ dysfunction (Singer et al., 2016). Sepsis pathogenesis includes metabolic alterations such as hypercatabolism, muscle wasting, and lipoatrophy (Kaneki, 2017), leading to cachexia characterized by decreased body weight, lean body mass, and fat mass as well as metabolic disruption and systemic inflammation (Evans et al., 2008; Argiles et al., 2010; Marques et al., 2013). Sepsis remains a leading cause of death in critically ill patients, with global estimates of 31.5 million cases resulting in 5.3 million deaths annually (Fleischmann et al., 2016). While advances in critical care have increased survival from acute sepsis, a growing number of patients progress to chronic critical illness that includes septic cachexia, a condition for which nutritional therapies have limited efficacy. Furthermore, there is currently no FDA-approved medication that specifically targets sepsis (Kaneki, 2017). Anti-inflammatory strategies are used to manage acute sepsis; however, no therapeutic approaches improve septic cachexia, and wasting of adipose tissue in sepsis has been largely unexplored (Callahan and Supinski, 2009; Schefold et al., 2010; Crowell et al., 2017).

Although adipose cachexia in sepsis is an understudied area, white adipose tissue (WAT) is known to be an important regulator of cachexia associated with cancer, with increases in WAT apoptosis, lipolysis, NLRP3 inflammasome activation, inflammatory cytokine expression, and decreases in adipogenesis and adipocyte size (Neves et al., 2016; Batista et al., 2013; Franco et al., 2017). Similarly, a recent study found that septic mice lost more weight than controls and failed to replete their fat mass even when body weight returned to baseline (Crowell et al., 2017). This state of septic adipose cachexia was associated with

* Corresponding author. Department of Pharmacology & Nutritional Sciences, Vice President for Research, University of Kentucky, Room 521b, Wethington Building, 900 S. Limestone, Lexington, KY, 40536-0200, USA.
E-mail address: lcassis@uky.edu (L.A. Cassis).

https://doi.org/10.1016/j.fct.2019.05.012
Received 25 March 2019; Received in revised form 7 May 2019; Accepted 8 May 2019
Available online 09 May 2019

increases in inflammation, apoptosis, and lipolysis, and decreases in lipogenesis of WAT (Crowell et al., 2017). These results suggest that adipose tissue is a site where cachexia from sepsis is manifest, but mechanisms for adipose tissue wasting during acute or chronic sepsis are not well defined.

Pseudomonas aeruginosa (*P. aeruginosa*) is a Gram-negative bacterium with a high propensity for antibiotic resistance that commonly colonizes the lung and gut and is a leading cause of sepsis. *P. aeruginosa* produces pyocyanin, a blue-pigmented toxin that is a major virulence factor for this organism. The toxic and inflammatory properties of pyocyanin are due, in part, to its ability to increase production of reactive oxygen species, induce neutrophil apoptosis, and facilitate the formation of biofilms (Singer et al., 2016; Caldwell et al., 2009; Hall et al., 2016; Jayaseelan et al., 2014). Pyocyanin possesses both antibiotic and antifungal properties, which allow it to kill off competitors of *P. aeruginosa.* The majority of studies on pyocyanin have focused on its ability to facilitate the virulence of *P. aeruginosa*.

Recent studies demonstrated that pyocyanin binds the aryl hydrocarbon receptor (AhR) and results in AhR activation in macrophages and pneumocytes (Moura-Alves et al., 2014). Pyocyanin has structural similarity to 2,3,7,8-tetrachlorodibenzodioxin (TCDD), a prototypical ligand of AhR, and similar to TCDD, easily crosses the cell membrane as a low molecular weight zwitterion (Singer et al., 2016). AhR-deficient mice are more susceptible to *P. aeruginosa* lung infection than wild type mice, indicating a role of AhR in resistance against *P. aeruginosa* that is potentially related to clearance of pyocyanin (Moura-Alves et al., 2014). In its classical role in drug and xenobiotic metabolism, AhR binds to xenobiotic response elements in the promoter regions of genes such as cytochrome P450 CYP1a1, CYP1a2, and CYP1b1 (Fujii-Kuriyama and Mimura, 2005). AhR exhibits promiscuous ligand binding to many drug and xenobiotic ligands, including persistent organic pollutants (POPs), such as TCDD and coplanar polychlorinated biphenyls (PCBs) (Singer et al., 2016). AhR has been implicated in the differentiation and functional regulation of several different cell types, including adipocytes. The functions of adipocyte AhR are of particular interest due to the lipophilicity of AhR ligands, including POPs, which results in their accumulation in adipose tissue in close proximity to adipocyte AhR (La Merrill et al., 2013).

Pyocyanin has been detected in sputum, wounds, and urine in concentrations up to 130 μM (Wilson et al., 1988; Cruickshank and Lowbury, 1953). While there are several studies demonstrating pyocyanin promotes the virulence of *P. aeruginosa*, levels of pyocyanin released by the bacteria may also regulate the function of mammalian cells, including activation of AhR in adipocytes, a cell type potentially related to cachexia of chronic sepsis. In this study, we defined effects of the novel AhR ligand pyocyanin on *in vitro* adipocyte differentiation and inflammation. We then used this information to establish an *in vivo* model of pyocyanin-induced cachexia in male and female C57BL/6J mice to elucidate possible mechanisms of pyocyanin's effects on the development of septic cachexia.

2. Methods

2.1. Growth and differentiation of 3T3-L1 cells

3T3-L1 mouse adipocytes were purchased from ATCC (catalogue number CL-173, ATCC, Manassas, VA). Cells were plated into 6-well plates at a seeding density of 10,000 cells/cm^2 and grown in pre-adipocyte expansion medium containing 90% Dulbecco's modified Eagle's medium (DMEM; Invitrogen, Carlsbad, CA), 10% Newborn Calf Serum (NCS, Gemini Bio-Products, Carlsbad, CA), and 1% penicillin/streptomycin. Cells (passage number 6 or lower) were grown to 100% confluence at 37 °C in a humidified 5% CO_2 atmosphere and culture media was changed every 48 h. Two days after cells reached 100% confluence, differentiation was initiated (day 0) with media containing 90% DMEM, 10% fetal bovine serum (FBS; Gemini Bio-Products, Woodland, CA), 1% penicillin/streptomycin, 0.2 μM insulin, 0.5 mM IBMX and 1.0 μM dexamethasone. Forty-eight hours later (day 2), media was changed to adipocyte maintenance media containing 90% DMEM, 10% FBS, 1% penicillin/streptomycin, and 0.2 μM insulin. Following day 2, media was changed every 48 h (day 4 and day 6) using maintenance media containing 90% DMEM, 10% FBS, and 1% penicillin/streptomycin. On day 8, cells were considered fully differentiated adipocytes.

2.2. Pyocyanin treatment in 3T3-L1 cells

Pyocyanin was purchased from Sigma-Aldrich (catalogue number P0046, Sigma-Aldrich, St. Louis, MO) and dissolved in DMSO. For treatment during differentiation, 3T3-L1 cells were grown to confluence in preadipocyte expansion medium in 6-well plates. Two days after reaching confluence, cells were treated with 0 (DMSO, 0.02%), 10, 50, or 100 μM pyocyanin, with fresh media containing vehicle or pyocyanin added on days 0, 2, 4, and 6. On day 8, cells were harvested for RNA extraction and gene expression analysis, or Oil Red O (ORO) staining as a marker of adipocyte differentiation. For post-differentiation treatment of mature adipocytes, fully differentiated 3T3-L1 adipocytes (day 8 cells) were treated with 0, 10, 50, or 100 μM pyocyanin for 24 h and then harvested for RNA extraction or ORO staining. Cells were scraped using 175 μL of RNA lysis buffer (Maxwell, catalogue # MC501C, Promega, Madison, WI), and stored at −80 °C. Oil Red O staining was performed on separate plates on day 8 or 9 using the ORO Staining Kit from Lifeline Cell Technology (catalogue number LL-0052, Frederick, MD). Stained cells were imaged at 100x. After imaging, water was removed from the stained cells, 500 μL of isopropanol was added to each well for 1 min to extract ORO from the cells, and 200 μL was removed from each well and absorbance measured in a 96-well plate at 510 nm in a spectrophotometer.

2.3. Animal treatments and sample collection

All experiments met the approval of the Animal Care and Use Committee of the University of Kentucky. Mice were housed in microisolator, polystyrene cages with a 14 h light/10 h dark cycle. Room temperature was at a range of 20–21 °C, and humidity ranged from 30 to 70%. Male and female mice C57BL/6J mice were purchased from The Jackson Laboratories (Bar Harbor, MA) and aged 6 months to have sufficient fat mass to assess adipose cachexia. All mice were fed standard murine diet (Harlan Teklad 2918 Global Rodent Diet, irradiated; Harlan Laboratories, Indianapolis, IN) *ad libitum* for the duration of the study design. Body weights were quantified daily. At study end point, mice were anesthetized [ketamine/xylazine, 10/100 mg/kg, by intraperitoneal (ip) injection] for exsanguination and tissue harvest (liver, subcutaneous adipose (SubQ), retroperitoneal adipose (RPF), epididymal adipose (EF)/periovarian fat (POF), interscapular brown adipose tissue (BAT), heart, lung, and soleus)).

2.4. Isolation of the stromal vascular fraction (SVF) from adipose

SubQ and EF tissue was aseptically excised from C57BL/6J mice, minced, and incubated in Omental basal medium (cat. no. OM-BM Zenbio, Research Triangle Park, NC) supplemented with collagenase (1 mg/mL) and penicillin (100 U/mL)/streptomyocin (100 μg/mL) for 1 h with shaking at 37 °C, as previously described in 12-well plates at a seeding density of 50,000 cells/cm^2 (Rodbell, 1964). Two days after SVF cells had reached 100% confluence (day 0), the medium was changed to differentiation media and then replaced every other day with fresh media for 8 days. Cells were harvested at day 8 after differentiation for ORO staining and RNA isolation using Maxwell RSC simplyRNA Cell Kit; cDNA synthesis and real-time PCR were performed as described below.

2.5. Pyocyanin treatment of stromal vascular cells (SVF) differentiated to adipocytes

SVF cells were harvested from naïve 10-month old male C57BL/6J mice and plated onto 12-well plates at a seeding density of 50,000 cells/cm^2. Cells were treated with vehicle (DMSO, 0.02%) or pyocyanin (100 μM) beginning on day 0 and every 48 h thereafter until cells were collected for ORO staining and RNA extraction on day 8.

2.6. Dose escalation pyocyanin pilot study in C57BL/6J mice

Male C57BL/6J mice, aged to 6 months as adults with significant adipose tissue mass, were administered vehicle (phosphate buffered saline, PBS) or escalating doses (2, 6, 19, and 50 mg/kg) of pyocyanin by intraperitoneal (IP) injection separated by 3–4 days. Body weights were recorded daily, and body composition was quantified by EchoMRI as described below. Study endpoint occurred 3 weeks after the final injection of 50 mg/kg pyocyanin.

2.7. Dose response pyocyanin pilot study in C57BL/6J mice

Male C57BL/6J mice (6 months of age) were administered three individual IP injections, given at weeks 0, 3 or 13, of PBS VEH control or pyocyanin at 30, 40, or 50 mg/kg. Body weights were recorded daily, and body composition was measured by EchoMRI as described below. Study endpoint occurred 24 h after the final injection.

2.8. Repeated pyocyanin administration to male C57BL/6J mice with tissue harvest 1 day following the last dose

Male C57BL/6J mice (6 months of age) were administered IP injections of PBS VEH control or pyocyanin (40 mg/kg, ip) on day 0 and 7, with study endpoint 24 h after the last dose. Body weights were quantified daily and EchoMRI was performed prior to each injection as described below. After each injection, body temperature was quantified using a subcutaneously implantable programmable temperature transponder (IPTT) and Bio Medic Data Systems (BMDS) transponder (product numbers IPTT 300 and DAS-7007, Bio Medic Data Systems Inc, Seaford, DE). At study endpoint, EF explants were prepared (described below) and SVF cells were isolated from both EF and SubQ for adipocyte differentiation.

2.9. Repeated pyocyanin administration to male and female C57BL/6J mice with tissue harvest 2 weeks following the last dose

Male and female C57BL/6J mice (6 months of age) were administered IP injections of PBS VEH control or pyocyanin (40 mg/kg, ip) on days 0, 7 and 14, with study endpoint two weeks after the final dose. Body weights were taken daily and EchoMRI was performed each week prior to the next injection. Male mice received their first two injections while in indirect calorimetry chambers (LabMaster TSE Systems Inc., Chesterfield, MO). After one week of acclimation to the chamber system, baseline measurements were recorded for one week. Mice received two injections of PBS or pyocyanin, separated by one week, while recordings continued for 7 days beyond the last injection. Data from three 24-h periods after each injection were adjusted for lean mass and averaged. For both sexes, study endpoint occurred two weeks following the third injection, at which point EF explants were used to quantify lipolysis (described below) and SVF cells were isolated from SubQ for adipocyte differentiation.

2.10. Measurement of body composition

Body composition (fat and lean mass) of conscious mice was determined by nuclear magnetic resonance spectroscopy [EchoMRI (magnetic resonance imaging)] as described previously (Baker et al., 2015).

2.11. Extraction of RNA and quantification of mRNA abundance by real-time PCR (RT-PCR)

Total RNA was extracted from tissues and cells using the Maxwell RSC simplyRNA Cell or Tissue Kit (Promega Corporation, Madison, WI) according to the manufacturer's instructions. RNA concentrations were determined using a NanoDrop 2000 spectophotometer (ThermoScientific, Wilmington, DE). cDNA was synthesized from 0.4 μg total RNA with qScript cDNA SuperMix (Quanta Biosciences, Gaithersburg, MD) in the following reaction: 25 °C for 5 min, 42 °C for 30 min, and 85 °C for 5 min. The cDNA was diluted to 0.4 ng/μL and amplified with an iCycler (Bio-Rad, Hercules, CA) and the Perfecta SYBR Green Fastmix for iQ (Quanta Biosciences, Gaithersburg, MD). Using the difference from GAPDH cDNA (reference gene) and the ΔΔCt method, the relative quantification of mRNA abundance in each sample was calculated. The PCR reaction was as follows: 94 °C for 5 min, 40 cycles at 94 °C for 15 s, 60 °C or 64 °C (based on tested primer efficiency) for 40 s, 72 °C for 10 min, and 100 cycles from 95 °C to 45.5 °C for 10 s. Primer sequences were as follows: *AhR*, forward 5′- GACCAA ACACAAGCTAGACTTCACACC, reverse 5′- CAAGAAGCCGGAAAACTG TCATGC; *AhR*, forward 5′-AGTAAAGCCCATCCCCGCTGAAGG-3′, reverse 5′-CATCAAAGAAGCTCTTGGCCC-3′; *CYP1A1 (cytochrome P450 1A1)*, forward 5′-AGTCAATCTGAGCAATGAGTTTGG-3′, reverse 5′-GGCATCCAGGGAAGAGTTAGG-3′; *GAPDH*, forward 5′-GCCAAAAG GGTCATCATCTC-3′, reverse 5′-GGCCATCCACAGTCTTCT-3′; *TNF-α*, forward 5′-CCCACTCTGACCCCTTTACTC-3′, reverse 5′-TCACTGTCCC AGCATCTTGT-3′; *aP2*, forward 5′- GGAACCTGGAAGCTTGTCTC-3′, reverse 5′- TGATGCTCTTCACCTTCCTG-3′; *PPARγ*, forward 5′- GATG GAAGACCACTCGCATT-3′, reverse 5′- AACCATTGGGTCAGCTCTTG-3′; *β-catenin*, forward 5′-ATGGACTGCCTGTTGTGGTT-3′, reverse 5′- AAA GGCGCATGATTTGCTGG-3′; *RANTES*, forward 5′- CCCTCACCATCATC CTCACT-3′, reverse 5′- CCTTCGAGTGACAAACACGA-3′; *F4/80*, forward 5′- CTTTGGCTATGGGCTTCCAGTC-3′, reverse 5′- GCAAGGAGG ACAGAGTTTATCGTG-3′.

2.12. Quantification of lipolysis in adipose tissue explants

Epididymal adipose tissue was cut into 25–50 mg explants. Each EF explant was placed into an individual well of a 24-well plate containing Krebs buffer (1 mL). Explants were washed with fresh buffer, which was removed and replaced with Krebs buffer (0.5 mL) containing 2% fatty acid free bovine serum albumin, and the plates were incubated at 37 °C. A 30 μL sample of buffer was removed from each well at 60, 120, 180, and 240 min after the start of the incubation. The glycerol concentration of the samples was quantified using the Glycerol Colorimetric Assay Kit (Item # 10010755, Caymen Chemicals, Ann Arbor, MI) per the manufacturer's instructions. The remaining EF explants were washed three times with Krebs buffer (1 mL/each) and frozen for protein determination. For protein determination, tissue samples were suspended on ice in PBS (0.5 mL) containing EDTA (2 mM) and protease cocktail inhibitor (cOmplete Mini, Roche Diagnostics, Indianapolis, IN). Tissue was homogenized using a Geno/Grinder (Spex SamplePrep, Metuchen, NJ) set to 1350 rpm × 1.5 min. After homogenization, samples were centrifuged at 14,000 rpm × 10 min at 4 °C and the supernatants transferred to clean tubes. Protein concentrations of the supernatants were determined using the Pierce BCA protein assay kit (Dallas, TX). Lipolysis is reported as amount of glycerol produced/mg protein/hour.

2.13. Quantification of plasma concentrations of inflammatory cytokines

Mouse plasma (25 μL) was collected in EDTA and diluted 1:2 in Assay Buffer (Milliplex, Item #L-AB, Millipore Sigma, Burlington, MA) to quantify plasma inflammatory cytokine concentrations using the

Mouse Cytokine/Chemokine Magnetic Bead Panel as per the manufacturer's instructions (Item #MCYTOMAG-70K-PMX, Millipore Sigma, Burlington, MA). The 96-well magnetic bead assay was read using a Luminex 200 (R&D Systems, Minneapolis, MN).

2.14. Quantification of pyocyanin concentrations in biological samples

Sample preparation: Plasma (50 μL) or adipose homogenate (200 mg/mL) was added to a 1.5 mL microcentrifuge tube. Internal standard solution (10 μL; caffeine-d_3, 100 ng/mL in ethanol) and ethanol (10 μL) were added (for calibration samples, 10 μL of ethanol containing pyocyanin in a concentration range of 2.5–625 ng/mL) to each tube. After briefly vortex-mixing, methanol (50 μL) and 10% perchloric acid solution (150 μL) were added and the contents mixed for 5 min. Tubes were centrifuged for 5 min at 11, 000 × *g*. The supernatant was recovered and transferred to an autosampler vial.

LC-MS/MS analysis: Analysis was performed on an AB Sciex 4000 Q Trap coupled with an Exion LC system. The Analyst software package was used for data collection and analysis. Chromatography was carried out with a C_8 reverse-phase column (Waters ACQUITY UPLC BEH C_8, 2.1 × 50 mm, 1.7 μm) maintained at 40 °C and the flow rate was set to 0.3 mL/min. Solvent A is 100% water with 0.1% formic acid and ammonium carbonate (5 mM) and solvent B is 90% methanol with 0.1% formic acid and ammonium carbonate. A gradient program was used as follow (T min/%A): 0/95, 1.0/95, 2.5/75, 5.0/75, 5.1/0, 6.6/0, 6.7/95, 9.0/95. The injection volume was 5.0 μL. Mass spectrometer was equipped with an electrospray ionization (ESI) source and operated in positive mode under the following operating parameters: IonSpray Voltage 5.5 kV, Desolvation temperature 500 °C, Ion Source Gas 1 40 psi, Ion Source Gas 2 40 psi, Curtain Gas 30 psi, Collision Gas Medium, Declustering Potential 80 V, Entrance Potential 10.0 V, and Collision Energy 27.0 V for caffeine and 45.0 V for pyocyanin. Quantitative analysis was conducted by monitoring the precursor ion to production ion transitions of m/z 211.2/168.2 for pyocyanin and m/z 198.2/138.0 for caffeine-d_3 with a dwell time of 0.15 s.

2.15. Metabolite identification of pyocyanin in mouse urine

Urine samples were extracted using methanol, and the supernatant was dried under nitrogen. After reconstituting in 90% acetonitrile, sample (2 μL) was injected for LC-MS analysis. A Q-Exactive mass spectrometer equipped with an Ultimate 3000 ultra high performance liquid chromatography system (Thermo Fisher Scientific, San Jose, CA) was used for sample detection. Chromatographic separation was performed on a reversed phase Kinetex C18 column (2.6 mm × 100 mm, 2.1 μm, Phenomenex, USA). Mobile phases were composed of acetonitrile (A) and water (B), both containing 0.1% formic acid. The column temperature was maintained at 40 °C, and the flow rate was set to 0.25 mL/min. Mass spectrometric detection was performed by electrospray ionization in positive ionization mode with source voltage maintained at 4.3 kV. The capillary temperature, sheath gas flow and auxiliary gas flow were set at 330 °C, 35 arb and 12 arb, respectively. Full-scan MS spectra (mass range m/z 75 to 1000) were acquired with resolution R = 70,000 and AGC target 1e6. MS/MS fragmentation was performed using high-energy C-trap dissociation with resolution R = 35,000 and AGC target 2e5. The stepped normalized collisional energy scheme was set at 30, 40, and 50. Raw data files acquired in full scan-ddMS2 mode were imported into Compound Discoverer™ software (v. 2.1; Thermo Fisher Scientific) to identify pyocyanin metabolites. The software detects chromatographic peaks, and the mass of the corresponding compound is compared with a list of generated theoretical metabolites. Potential metabolites were proposed based on exact mass, MS2 fragmentation, isotopic pattern and retention time with respect to the parent compound.

2.16. Statistical analysis

Data are represented as mean ± SEM. Data were tested for normality using the Shapiro-Wilk test, and equal variance was tested using the Brown-Forsythe test. Outlier detection was performed using Grubbs' or extreme studentized deviate method where alpha = 0.05. If data did not pass normality using these approaches, data were logarithmically transformed. One-way analysis of variance (ANOVA; SigmaPlot, version 13.0; Systat Software Inc., Chicago, IL) was used to define effects of pyocyanin treatment *in vitro*. Dunnett's method was used for post-hoc analyses. T-tests were used to analyze *in vivo* comparisons between pyocyanin (PYO) and vehicle (VEH) treated animals. Body weights and body composition were analyzed by repeated measure. Body temperature analyses were performed in SAS 9.4 (SAS Institute Inc.; Cary, NC, USA). For each mouse, temperature was plotted against log-transformed time and the area under the curve (AUC) was calculated for each of the two injections. A full factorial two-way repeated measures ANOVA was performed on the AUC values, analyzing differences between across treatment and injection number. A Kenward and Roger adjustment was used to correct for small-sample bias. Post-hoc two-sample t-tests were performed at each timepoint, separated by injection number. Statistical significance was defined as $p < 0.05$.

3. Results

3.1. Pyocyanin reduces differentiation of 3T3-L1 cells to adipocytes

Previous studies demonstrated that activation of AhR reduced differentiation of 3T3-L1 cells to adipocytes (Alexander et al., 1998; Arsenescu et al., 2008; Phillips et al., 1995). Pyocyanin has been demonstrated to bind to AhR (Moura-Alves et al., 2014). Thus, we first defined concentration-dependent effects of pyocyanin (0–100 μM) on differentiation of 3T3-L1 cells to adipocytes. Pyocyanin (100 μM) reduced significantly ORO absorbance and staining as a marker of adipocyte differentiation compared to vehicle controls (Fig. 1A and B, $P < 0.05$). Similarly, mRNA abundance of Ap2 and PPARγ, genes associated with a mature adipocyte phenotype (Moseti et al., 2016), were reduced significantly by pyocyanin (100 μM; Fig. 1C, $P < 0.05$). As an index of AhR activation, pyocyanin resulted in robust increase in mRNA abundance of AhR and its downstream marker, CYP1a1 (Fig. 1C, $P < 0.05$). When incubated with differentiated adipocytes, pyocyanin (50, 100 μM) reduced significantly ORO absorbance and staining (Fig. 1D and E, $P < 0.05$). However, in mature adipocytes, while pyocyanin at high concentrations (100 μM) increased mRNA abundance of AhR, there was a non-monotonic, inverted-U shape dose response for effects of pyocyanin on mRNA abundance of CYP1a1 and TNF-α (Fig. 1F). Pyocyanin, at any concentration examined, did not significantly influence cell viability as quantified by trypan blue staining (data not shown).

3.2. Pyocyanin reduces differentiation of mouse adipose stromal vascular cells to adipocytes, and promotes lipolysis of mouse white adipose explants

We isolated the stromal vascular fraction (SVF) from adipose tissue to obtain stem cells as an alternative *in vitro* model of adipocyte differentiation. Similar to effects of pyocyanin to reduce differentiation of 3T3-L1 cells to adipocytes, pyocyanin (100 μM) reduced significantly ORO absorbance compared to vehicle controls after 8 days of the differentiation protocol (Fig. 2A, $P < 0.05$). Since pyocyanin reduced ORO absorbance when incubated with mature adipocytes (Fig. 1D), we defined effects of pyocyanin on lipolysis using epididymal (EF) white adipose explants from naïve male C57BL/6J mice. Following a 4 h incubation, pyocyanin (100 μM) increased significantly glycerol release from adipose tissue explants (Fig. 2B, $P < 0.05$).

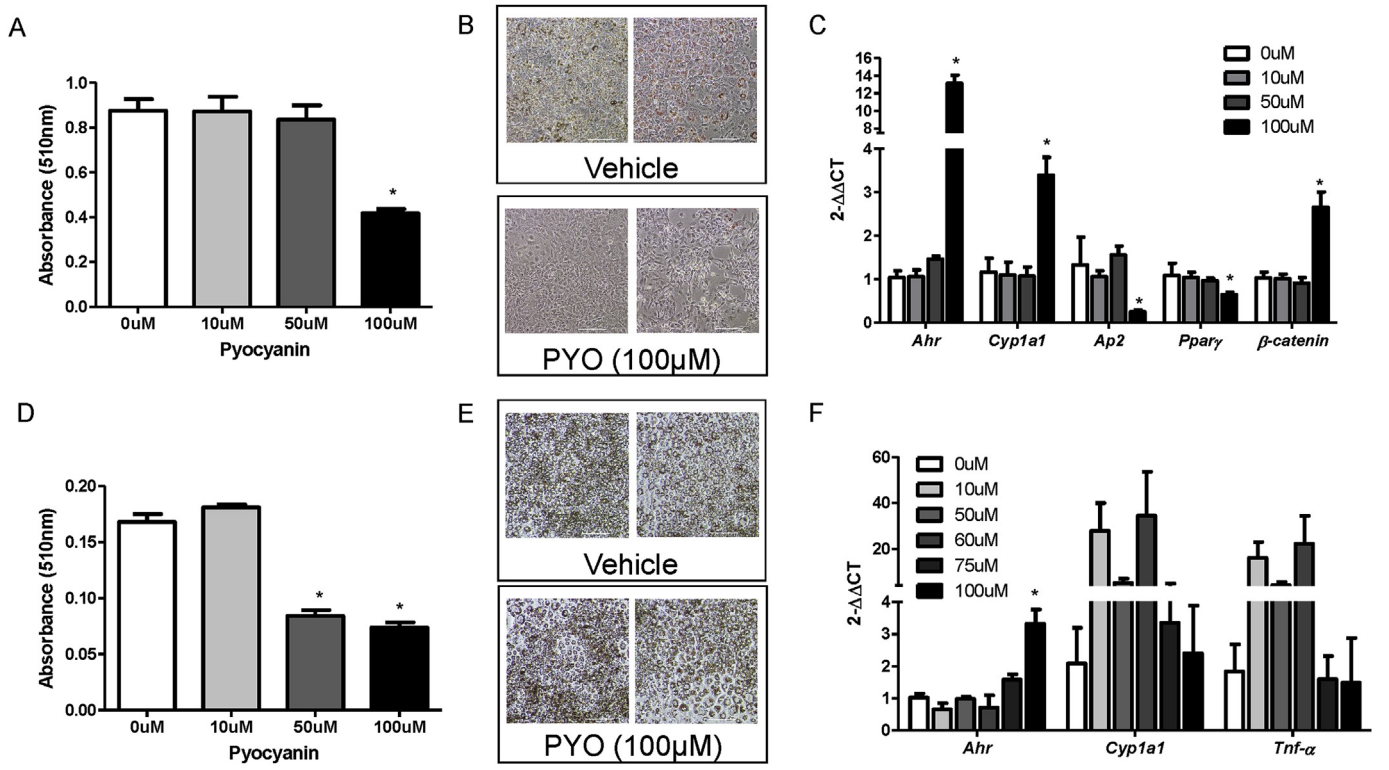

Fig. 1. Pyocyanin reduces *in vitro* adipocyte differentiation and induces markers of AhR activation in 3T3-L1 adipocytes. (A) Oil Red O (ORO) absorbance (510 nm, day 8 of differentiation protocol) of 3T3-L1 adipocytes treated with vehicle (0 μM) or pyocyanin. (B) Representative images of cells (day 8 from (A)) incubated with vehicle or pyocyanin (PYO). (C) mRNA abundance of AhR, CYP1a1, aP2, PPARγ, or β-catenin in 3T3-L1 adipocytes incubated with vehicle (0 μM) or pyocyanin during the differentiation protocol. (D) ORO absorbance of differentiated (day 8) 3T3-L1 adipocytes incubated with vehicle (0 μM) or pyocyanin for 24 h. (E) Representative images of differentiated 3T3-L1 adipocytes from (D) incubated with vehicle or pyocyanin. (F) mRNA abundance of AhR, CYP1a1, or TNF-α mRNA abundance in differentiated 3T3-L1 adipocytes incubated with vehicle (0 μM) or pyocyanin for 24 h. Scale bar in (B) and (E) is 200 μm. Data are mean ± SEM from n = 3–8 wells/treatment. *, P < 0.05 compared to 0 μM (VEH). (For interpretation of the references to colour in this figure legend, the reader is referred to the Web version of this article.)

3.3. Development of an in vivo model of pyocyanin-induced cachexia

We developed an *in vivo* model of pyocyanin-induced cachexia using adult male C57BL/6J mice (aged to 6 months to have sufficient fat mass to quantify adipose cachexia). Intraperitoneal (IP) injection of pyocyanin was chosen as a mode of delivery to replicate gut-derived sepsis. Initial dose escalation studies, initiated at 2 mg/kg of pyocyanin, had no effect on body weight, and thus doses were escalated to a maximum of 50 mg/kg of pyocyanin, which resulted in a reduction in body weight within 48 h after administration (34.1 ± 0.9 g at baseline versus 31.9 ± 1.2 g, $P < 0.05$). We then performed dose response studies testing effects of repeated exposures (two injections separated by one week) to 30, 40, and 50 mg/kg pyocyanin. During the course of these studies, we found that there is an effect of repeated exposures to pyocyanin, with greater losses in body weight and fat mass following a second injection of pyocyanin (see supplemental material, Figs. S1A and B). Furthermore, upon second injection with pyocyanin, mice exhibited changes in behavior, including lethargy, trembling, and poor motor control, which persisted for several hours after injection but returned to normal function within 12 h. We detected pyocyanin in plasma 24 h following the second injection of each dose (see supplemental material, Fig. S1C).

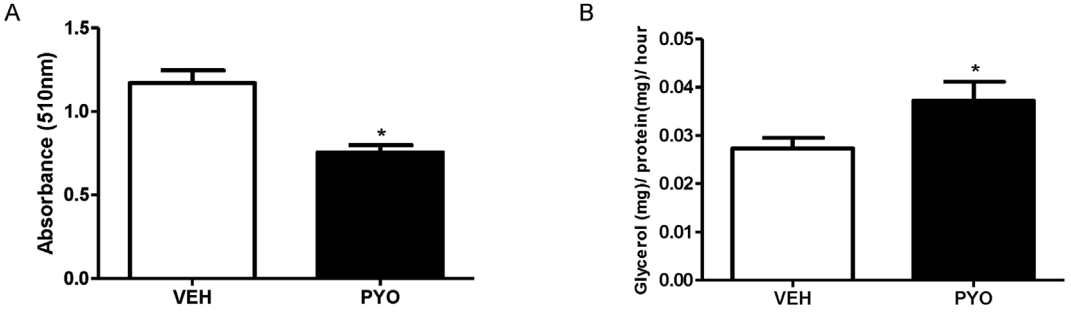

Fig. 2. Pyocyanin reduces adipocyte differentiation from murine stem cells and induces *ex vivo* lipolysis of mouse adipose explants. (A) Oil Red O (ORO) absorbance (510 nm) of adipocytes, incubated with vehicle (VEH) or pyocyanin (PYO, 100 μM), differentiated from the stromal vascular fraction (SVF) of mouse adipose tissue. (B) *Ex vivo* lipolysis (glycerol release) of epididymal adipose tissue explants incubated with vehicle (VEH) or pyocyanin (100 μM). Data are mean ± SEM from n = 9–10 mice/group. *, P < 0.05 compared to VEH.

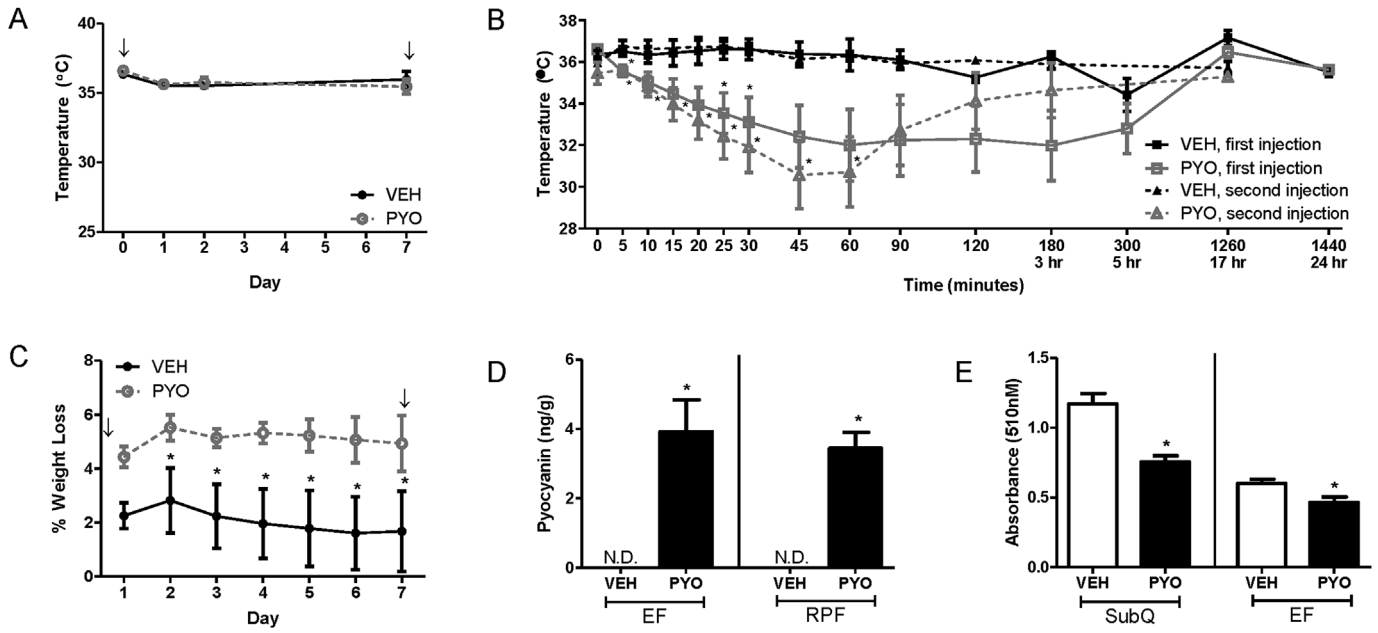

Fig. 3. Pyocyanin results in an acute reduction in body temperature and sustained reductions in body weight of male C57BL/6 mice. Mice received two IP injections of vehicle (VEH) or pyocyanin (PYO, 40 mg/kg) one week apart with study endpoint occurring 24-h after the second injection. (A) Subcutaneous body temperature measured at the same time of day for 7 days. (B) Subcutaneous body temperature measured over a 24-h period following the first or second IP injection. (C) Percent weight loss (original weight – current weight/original weight x 100) over 7 days. (D) Pyocyanin concentration in adipose tissues (epididymal, EF or retroperitoneal, RPF) 24 h after second injection. (none detected, N.D.) (E) Oil Red O absorbance (510 nm) of adipocytes (day 8) differentiated from SVF of subcutaneous (SubQ) or EF tissue (right) of mice administered vehicle or pyocyanin. ↓, indicates timing of IP injection. Data are mean ± SEM from n = 5–12 mice/group. *, P < 0.05 compared to VEH.

3.4. Pyocyanin acutely reduces body temperature and results in a sustained decrease in body weight, fat mass, and adipocyte differentiation in male C57BL/6J mice

Based on results from pilot studies, we administered two injections (IP) of pyocyanin (40 mg/kg) separated by one week. Moreover, because of the behavioral effects of the virulence factor in pilot studies, we quantified body temperature during the first 24 h after administration of each dose of pyocyanin, and then subsequently for 7 days at the same time each day. Both first and second injection of pyocyanin resulted in a rapid and robust decrease in body temperature (Fig. 3B, $P < 0.05$) that was accompanied by lethargy, trembling, and poor motor control. Calculation of the area under the curve for body temperature reductions during the 24 h following pyocyanin exposure demonstrated significant reductions compared to vehicle controls (data not shown). Pyocyanin-induced acute reductions in body temperature were not maintained beyond 24 h (Fig. 3B, $P < 0.05$), and body temperature was not significantly influenced by pyocyanin on subsequent days (Fig. 3A).

Normalization of body temperature coincided with a return to normal behavior and motor control. Acute body temperature-regulating effects of pyocyanin occurred prior to reductions in body weight (illustrated as % weight loss compared to baseline body weight) of pyocyanin-treated mice compared to vehicle controls (Fig. 3C). However, while body temperature quickly returned to normal within 24 h after injection (Fig. 3A and B), weight loss following pyocyanin was sustained throughout the 7 day time course (Fig. 3C). Pyocyanin was detected in the plasma 24 h following the second injection (PYO: 4.5 ± 1.0 ng/mL; VEH: none detected). We also quantified pyocyanin and associated metabolites in the urine of mice from this study. Pyocyanin was detected in urine (45 and 60 min post-injection) as the parent compound and five major metabolites (N-demethylation + glucorindation and oxidation + glucoronidation conjugates; See supplemental material, Fig. S2). Peak areas for each conjugate decreased from 45 to 60 min, indicating pyocyanin is rapidly metabolized. Additionally, while pyocyanin levels were non-detectable in adipose tissue from vehicle-treated animals, pyocyanin (4 ng/g) was detected in EF and RPF at 24 h after the last dose (Fig. 3D, $P < 0.05$).

EF explants removed from animals 24 h after the last dose of pyocyanin did not exhibit differences in basal lipolysis (See supplemental material, Fig. S2). Concentrations of the pro-inflammatory cytokine interleukin-6 (IL-6) were increased in plasma of mice administered pyocyanin compared to vehicle controls, while concentrations of the anti-inflammatory cytokine interleukin-13 (IL-13) were decreased compared to controls (Table 2, $P < 0.05$). There was a trend toward reduced plasma concentrations of interleukin-1 alpha (IL-1α) and increased concentrations of chemokine (C-X-C motif) ligand 1 (CXCL1) (Table 2). In adipose tissue, mRNA abundance of the T-cell marker, RANTES, was increased significantly 24 h after the last dose of pyocyanin (See supplemental material, Fig. S2, $P < 0.05$). However, there was no effect of pyocyanin on mRNA abundance of CYP1a1, PPARγ, aP2, TNF-α, F4/80, RANTES, or interleukin-10 (IL-10) in EF, RPF, or liver compared to vehicle controls (See supplemental material, Fig. S2).

We harvested SVF from subcutaneous and EF adipose tissue of mice administered vehicle or pyocyanin and differentiated stem cells *in vitro* to adipocytes. On day 8 of the differentiation protocol, ORO absorbance was decreased significantly in adipocytes differentiated from stem cells isolated from both adipose depots of pyocyanin-treated mice compared to vehicle controls (Fig. 3E, $P < 0.05$).

3.5. Pyocyanin chronically decreases body weight and fat mass of male C57BL/6J mice

In this study, we administered three injections (IP) of vehicle or pyocyanin (40 mg/kg) one week apart and harvested tissues 14 days after the last dose. Our goal was to determine if effects of pyocyanin to decrease body weight and fat mass of male mice were sustained two weeks after the last dose. Moreover, to resolve mechanisms for effects of pyocyanin, we quantified measures of whole-body metabolism following the first two injections of pyocyanin. We quantified food intake,

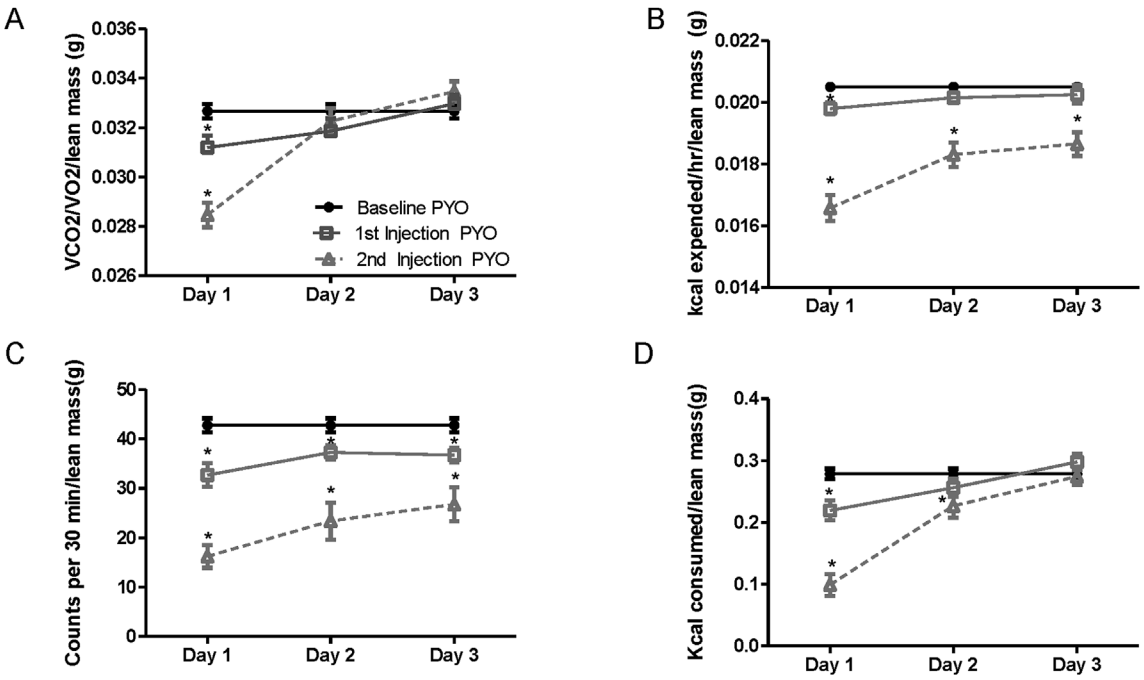

Fig. 4. Pyocyanin regulates indices of whole body metabolism in male mice. Indirect calorimetry collected over three days of baseline and the first three days following the first and second injection of pyocyanin (PYO) measuring (A) Respiratory exchange ratio (RER, VCO2/VO2/lean mass), (B) energy expenditure (kcal expended/hr/lean mass), (C) physical activity (counts/30 min/lean mass), or (D) energy intake (kcal consumed/lean mass). Data are mean ± SEM from n = 15 mice/timepoint. *, P < 0.05 compared to baseline PYO.

indirect calorimetry, and physical activity for 3 consecutive days at baseline (prior to exposure) and the 3 days following both the first and second injections of pyocyanin while mice were within the recording chambers. There were no changes in any measured parameter of vehicle-treated mice at any time point (data not shown). Thus, data are illustrated for pyocyanin-treated mice only. The first injection of pyocyanin resulted in significant reductions in respiratory exchange ratio (RER, as quantified by VCO_2/VO_2, Fig. 4A, *P < 0.05*), energy expenditure (kcal expended; Fig. 4B, *P < 0.05*), physical activity (counts/30 min; Fig. 4C, *P < 0.05*), and food intake (kcal consumed; Fig. 4D, P < 0.05) on day 1 of recording. With the exception of physical activity and energy expenditure, reductions in these parameters (RER, EE, food intake) returned to baseline levels by the second day following the initial injection of pyocyanin. Following the second injection of pyocyanin, there were more pronounced and sustained reductions in RER, EE, activity, and food intake (Fig. 4A–D, P < 0.05).

Male mice began losing weight following the second injection of pyocyanin and weighed significantly less than vehicle controls following the third injection of pyocyanin (Fig. 5A, P < 0.05). Similarly, lean mass (as a percentage of body weight) of pyocyanin-treated mice was increased significantly compared to vehicle controls, while fat mass was decreased significantly following the second injection of pyocyanin (Fig. 5B and C, P < 0.05).

At 14 days following the final dose, pyocyanin-treated mice had significant reductions in the mass (adjusted to body weight) of EF, retroperitoneal fat (RPF), and interscapular brown fat (isBAT) compared to vehicle controls (Table 1, P < 0.05). Liver mass was also reduced significantly in mice administered pyocyanin compared to vehicle controls (Table 1, *P < 0.05*). Lipolysis of EF explants was increased significantly at 14 days after the last injection of pyocyanin compared to vehicle controls (Fig. 5D, P < 0.05). Concentrations of IL-10 were reduced significantly in plasma from mice administered pyocyanin compared to vehicle controls (Table 2). Notably, pyocyanin resulted in a significant increase in mRNA abundance for CYP1a1 in EF and RPF, but not in liver (Fig. 5E, *P < 0.05*). Moreover, mRNA abundance of TNF-α was reduced significantly in RPF from mice administered pyocyanin compared to vehicle controls (Fig. 5E, *P < 0.05*). However, other markers of adipocyte differentiation (aP2, PPARγ), inflammation (TNF-α), macrophage infiltration (F4/80), or T-cell infiltration (RANTES) were not altered in adipose tissue from pyocyanin-treated mice. Moreover, absorbance of ORO in adipocytes differentiated from stem cells isolated from subcutaneous adipose tissue of mice administered pyocyanin was not significantly different from control (Fig. 5F), nor were there any differences in mRNA abundance of adipocyte markers in differentiated adipocytes (Fig. 5G). Effects of pyocyanin to promote basal lipolysis of adipose explants and activate CYP1a1 expression in adipose tissue were observed despite an inability to detect pyocyanin in plasma or adipose at 14 days after the last injection.

3.6. Pyocyanin chronically decreases body weight and fat mass of female C57BL/6J mice

Studies have demonstrated sex differences in sepsis incidence between males and females (Rhee et al., 2017; Martin et al., 2003). Thus, we repeated chronic pyocyanin exposures using the same experimental design as described above (with the exception of indirect calorimetry) in adult female C57BL/6 mice. In contrast to males, female mice began losing body weight after the first injection of pyocyanin compared to vehicle controls, and weight loss was maintained throughout the study protocol (Fig. 6A, P < 0.05). Body weight reductions were associated with increased lean mass and decreased fat mass compared to baseline levels within each treatment group, or compared to vehicle controls (Fig. 6B and C, P < 0.05). In females, pyocyanin's effect to reduce fat mass exhibited similar trends as seen in males, with modest reductions in weights of some fat pads compared to vehicle controls (Table 1). However, in contrast to males, liver mass of pyocyanin-treated female mice was increased significantly compared to vehicle controls (Table 1, *P < 0.05*). Moreover, in females, there was no significant effect of pyocyanin on lipolysis of adipose tissue explants compared to vehicle controls (Fig. 6D, *P < 0.05*). Similar to males, pyocyanin resulted in a significant increase in mRNA abundance of CYP1a1 in adipose tissue

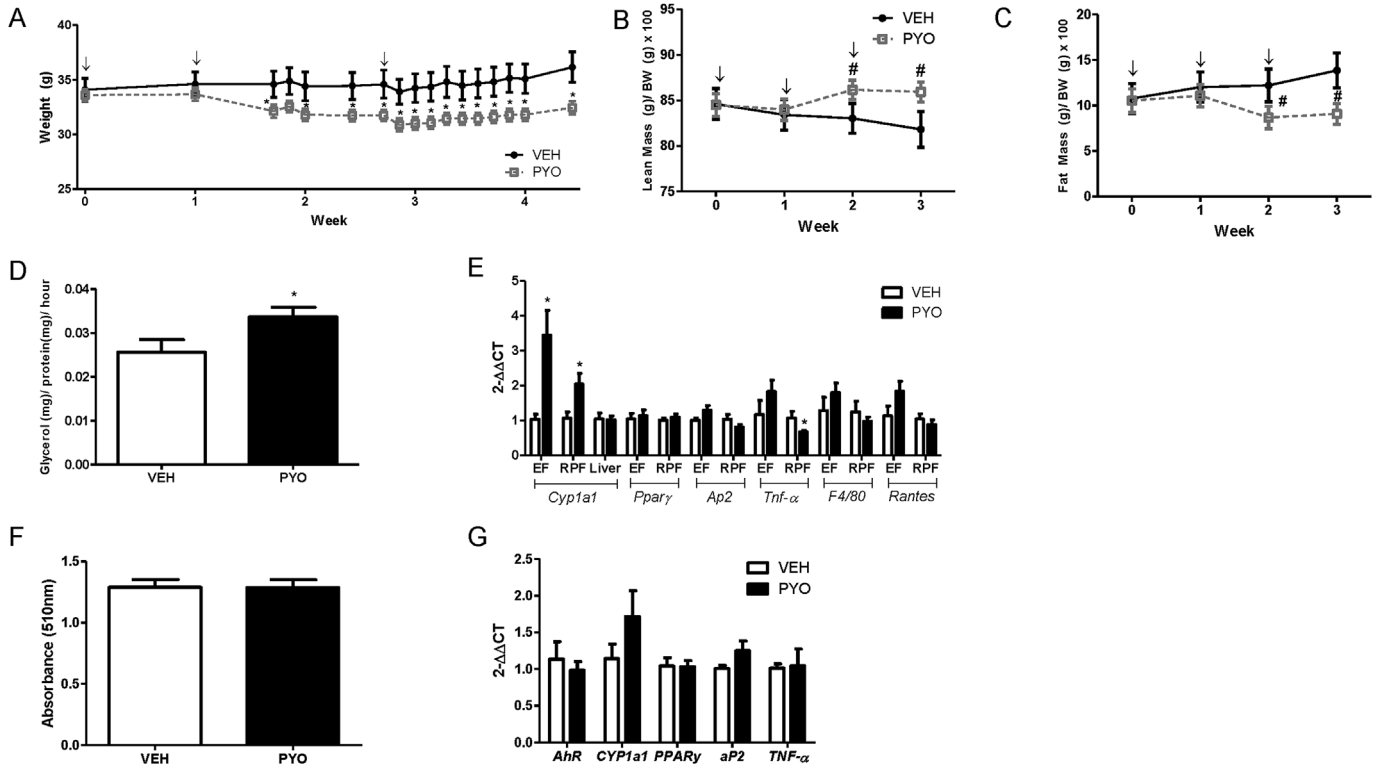

Fig. 5. Pyocyanin results in sustained reductions in body weight, lean and fat mass of male C57BL/6J mice. Male mice received three IP injections of vehicle (VEH) or pyocyanin (40 mg/kg) one week apart with study endpoint occurring 2 weeks after the third injection. (A) Body weights (g). (B) Percent lean mass (lean mass (g)/ body weight (g) x 100)). (C) Percent fat mass (fat mass (g)/body weight (g) x 100)). (D) *Ex vivo* lipolysis of EF explants as quantified by glycerol release. (E) mRNA abundance of target genes in EF, RPF, and liver. (F) Oil Red O (ORO) absorbance (510 nm) of adipocytes differentiated from SVF cells of male mice administered vehicle (VEH) or pyocyanin (PYO). (G) mRNA abundance of target genes in adipocytes differentiated from (F). ↓, indicates timing of IP injection. Data are mean ± SEM from n = 5–15 mice/group. *, P < 0.05 compared to VEH. #, P < 0.05 as compared to baseline pyocyanin.

but not in livers of female mice compared to vehicle controls, with no changes in mRNA abundance of aP2 or PPARγ (Fig. 6E, *P < 0.05*). Pyocyanin resulted in a significant decrease in RANTES mRNA abundance in periovarian adipose tissue compared to vehicle controls (Fig. 6E, *P < 0.05*). Moreover, pyocyanin resulted in a significant decrease in RANTES plasma concentrations of females compared to vehicle controls (Table 2, *P < 0.05*).

Notably, while there were no significant differences in ORO absorbance when SVF cells isolated from pyocyanin-treated females were differentiated *in vitro* to adipocytes (Fig. 6F), adipocytes differentiated from pyocyanin-treated females exhibited significant elevations in mRNA abundance of AhR and TNF-α (Fig. 6G, *P < 0.05*). These effects were observed in cells isolated two weeks after the last injection, when pyocyanin levels in plasma and adipose were below the detectable limit.

4. Discussion

Results from these studies demonstrate that pyocyanin, a virulence factor released by the sepsis-causing bacteria *P. aeruginosa*, regulates adipocyte formation and function *in vitro*, and regulates body weight of male and female mice *in vivo*. Specifically, we found that (1) pyocyanin reduces differentiation of adipocytes, promotes expression of inflammatory cytokines in differentiated adipocytes, and augments basal lipolysis of adipose tissue explants, (2) pyocyanin results in reductions in body weight and fat mass when administered *in vivo* to both male and

Table 1
Effect of *in vivo* pyocyanin administration on tissue weights of male and female mice.

Tissue	Tissue weight (g)/Body weight (g)					
	Acute Males		Chronic Males		Chronic Females	
	Vehicle	Pyocyanin	Vehicle	Pyocyanin	Vehicle	Pyocyanin
EF	0.043 ± 0.008	0.042 ± 0.01	0.028 ± 0.007	0.019 ± 0.007 *	0.025 ± 0.0112	0.017 ± 0.003
SubQ	0.019 ± 0.008	0.019 ± 0.006	0.009 ± 0.002	0.008 ± 0.003	0.011 ± 0.0033	0.011 ± 0.0022
RPF	0.015 ± 0.003	0.013 ± 0.002	0.010 ± 0.003	0.006 ± 0.003 *	0.005 ± 0.003	0.003 ± 0.0006
isBAT	0.006 ± 0.002	0.007 ± 0.002	0.006 ± 0.0008	0.005 ± 0.0003 *	0.005 ± 0.00097	0.004 ± 0.0007
Liver	0.046 ± 0.002	0.045 ± 0.006	0.056 ± 0.003	0.051 ± 0.003 *	0.041 ± 0.0061	0.048 ± 0.0028 *
Lung	0.006 ± 0.003	0.006 ± 0.002	0.006 ± 0.002	0.006 ± 0.0009	0.006 ± 0.0015	0.008 ± 0.0031
Heart	0.004 ± 0.001	0.004 ± 0.001	0.005 0.0003	0.005 0.0004	0.005 ± 0.0009	0.005 ± 0.0003
Soleus	0.0006 ± 0.0001	0.0006 ± 0.0001	–	–	0.0006 ± 0.00009	0.00071 ± 0.0001 *

Values are mean ± SEM from n = 5–15/group. *, P < 0.05 compared to vehicle.
Abbreviations: EF, epididymal fat; SubQ, subcutaneous fat; RPF, retroperitoneal fat; isBAT, interscapular brown fat.

Table 2
Plasma cytokine concentrations in male and female mice administered vehicle or pyocyanin.

Cytokine	Plasma Cytokine Concentration (pg/mL)					
	Acute Males		Chronic Males		Chronic Females	
	Vehicle	Pyocyanin	Vehicle	Pyocyanin	Vehicle	Pyocyanin
IL-1α	67.20 ± 35.05	31.21 ± 12.91	31.22 ± 32.82	21.91 ± 9.41	35.31 ± 22.75	19.87 ± 15.29
IL-6	8.14 ± 5.52	33.03 ± 18.69*	0.65 ± 0.48	0.93 ± 1.13	0.78 ± 0.86	1.65 ± 1.97
IL-13	27.34 ± 8.15	9.54 ± 8.61*	18.36 ± 12.74	13.94 ± 9.72	15.75 ± 13.04	49.07 ± 71.13
IL-10	2.68 ± 2.51	2.32 ± 1.98	5.59 ± 3.68	3.41 ± 0.93*	3.73 ± 3.83	4.24 ± 3.64
IP-10	148.95 ± 72.50	130.57 ± 45.74	139.73 ± 32.86	115.89 ± 11.81	105.62 ± 23.03	124.39 ± 40.94
CXCL1	44.94 ± 21.11	132.63 ± 102.54	27.58 ± 11.61	41.09 ± 30.87	25.14 ± 12.21	17.28 ± 10.99
RANTES	17.91 ± 10.48	9.86 ± 5.47	5.02 ± 4.99	6.46 ± 3.34	11.93 ± 5.33	5.21 ± 3.56*

Values are mean ± SEM from n = 5–15/group. *, P < 0.05 compared to vehicle.

female mice, (3) there are sex differences in mechanisms related to effects of pyocyanin on adipose tissue. While there has been a growing interest in the role of the virulence-promoting effects of pyocyanin in sepsis following *P. aeruginosa* infection, the role of pyocyanin at mammalian cells such as adipocytes in the wasting and cachexia associated with sepsis has been largely unexplored. Our results suggest that pyocyanin exerts long-lasting effects to regulate body weight, adipose mass, and adipocyte function. These findings may have relevance to the wasting associated with chronic sepsis.

Using 3T3-L1 cells, we found that pyocyanin stimulated expression of CYP1a1 as an index of AhR activation at concentrations (100 μM) that resulted in a 50% reduction in adipocyte differentiation. Notably, this concentration of pyocyanin has been detected in human samples (Wilson et al., 1988; Cruickshank and Lowbury, 1953). Our laboratory has reported previously an ability of AhR ligands, including coplanar PCBs and dioxin (TCDD), to reduce adipocyte differentiation (Arsenescu et al., 2008). In agreement with these findings, pyocyanin reduced several indices of adipocyte differentiation at concentrations that induced markers of AhR activation in 3T3-L1 adipocytes. While pyocyanin elicited downstream markers of AhR activation in adipocytes, it is unclear if the effects of pyocyanin on adipocytes were AhR-mediated.

In mature adipocytes, pyocyanin also reduced ORO staining and promoted expression of TNF-α. Elevations in mRNA abundance of proinflammatory adipokines in response to pyocyanin is in agreement with previous findings of adipocyte inflammation following treatment with AhR agonists in 3T3-L1 adipocytes (Arsenescu et al., 2008). It is interesting to note pyocyanin's effect on CYP1a1 and TNF-α mRNA abundance in mature adipocytes appears to follow a non-monotonic,

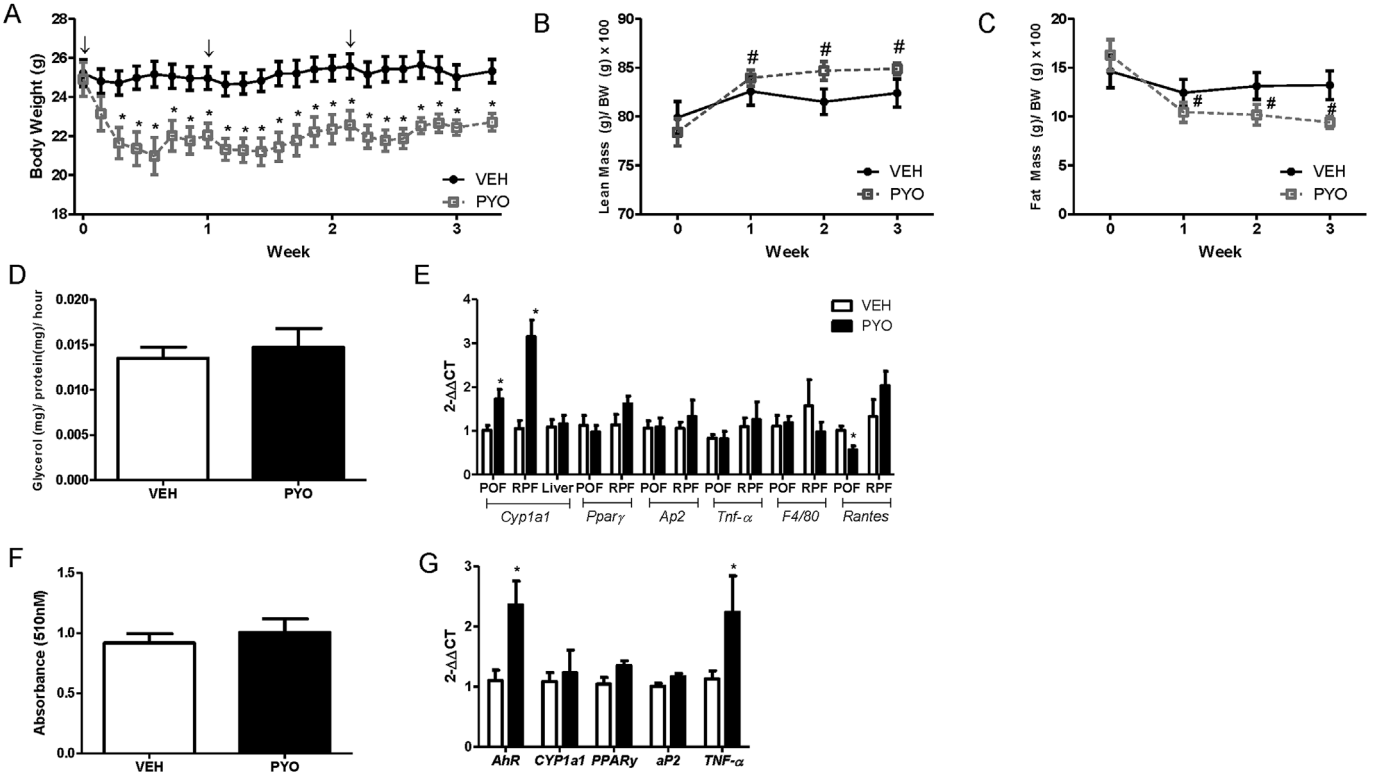

Fig. 6. Pyocyanin results in sustained and robust reductions in body weight, lean and fat mass of female C57BL/6J mice. Female mice received three IP injections of vehicle (VEH) or pyocyanin (PYO, 40 mg/kg) one week apart with study endpoint occurring 2 weeks after the third injection. (A) Body weights (g). (B) Percent lean mass (lean mass (g)/body weight (g) x 100)). (C) Percent fat mass (fat mass (g)/body weight (g) x 100)). (D) *Ex vivo* lipolysis of EF explants as quantified by glycerol release. (E) mRNA abundance of CYP1a1, PPARγ, aP2, TNF-α, F4/80, or RANTES in EF, RPF, and liver. (F) Oil Red O (ORO) absorbance (510 nm) of adipocytes differentiated from SVF cells of male mice administered vehicle (VEH) or pyocyanin (PYO). (G) mRNA abundance of target genes in adipocytes differentiated from (F). ↓, indicates timing of IP injection. Data are mean ± SEM from n = 5 mice/group. *, P < 0.05 compared to VEH. #, P < 0.05 as compared to baseline pyocyanin.

inverted-U shaped dose response, with the greatest inductions of gene expression occurring at intermediate concentrations of pyocyanin. We have previously reported that AhR ligands, namely environmental pollutants, exhibit non-monotonic and inverted U-shaped associations with disease outcomes (Jackson et al., 2017). A reduction in ORO staining of mature adipocytes exposed to pyocyanin may represent an increase in lipolysis, potentially related to induction of TNF-α (Sharma and Puri, 2016; Souza et al., 2003). Indeed, using adipose tissue explants from mice, we demonstrated that pyocyanin increased basal lipolysis. In a parallel adipocyte differentiation system using stem cells harvested from naïve mice, pyocyanin (100 μM) again decreased markers of adipocyte differentiation. Therefore, it appears pyocyanin might have contrasting effects on pre-/differentiating adipocytes *versus* mature adipocytes, representing an important consideration when interpreting *in vivo* data and defining future therapeutic targets.

Based on these *in vitro* findings, we developed an *in vivo* model of pyocyanin-induced cachexia that did not include use of the parent bacteria, as *P. aeruginosa* produces additional phenazines that could confound the effects of pyocyanin on mammalian cells. Utilizing IP injection to replicate potential pyocyanin exposures from gut-derived sepsis, pyocyanin dose-dependently elicited sustained weight loss upon repeated exposures. Moreover, while an initial injection of pyocyanin had no effects in male mice, several effects were noted upon second injection, including short-lived behavioral changes. Our findings are in agreement with previous studies indicating that intranasal exposure to pyocyanin resulted in reduced spontaneous locomotor activity and increased immobility time in forced swim (Arora et al., 2018). Moreover, hypothermia is a known symptom of sepsis (Remick and Xioa, 2006). Our results demonstrate that behavioral effects of pyocyanin, including lethargy, trembling, and poor motor control, were associated with a rapid decrease in body temperature that returned to baseline levels 17 h after injection, when behavioral effects were no longer evident. These results suggest that hypothermia, trembling, and disorientation associated with sepsis from *P. aeruginosa* may result from release of pyocyanin from the bacteria. However, since weight loss from pyocyanin exposure was sustained and did not coincide with the timeframe for behavioral or temperature-regulating effects of the compound, these results suggest that other mechanisms contribute to pyocyanin's effects on body weight.

To elucidate mechanisms contributing to body weight-regulating effects of pyocyanin, we studied its effects on adipocyte differentiation and adipose inflammation. Remarkably, when stem cells were harvested 24 h after the last dose of pyocyanin and differentiated over an 8 day experimental protocol, markers of adipocyte differentiation were reduced, suggesting long-lasting effects of pyocyanin. It is noteworthy that mice injected with pyocyanin begin metabolizing and excreting the compound through their urine within 45 min of injection; however, pyocyanin was still detectable in the plasma and adipose at 24 h, when stem cells were harvested for *in vitro* adipocyte differentiation. Plasma concentrations of the pro-inflammatory cytokine IL-6 were increased 24 h after the last dose of pyocyanin, while concentrations of the anti-inflammatory cytokine IL-13 were decreased in pyocyanin-treated mice. Elevations in systemic IL-6 concentrations have been demonstrated in patients with sepsis (Hotchkiss et al., 2013; Minasyan, 2017; Tsalik et al., 2012), with high IL-6 levels associated with poor outcomes in sepsis (Cavaillon et al., 2003; Chousterman et al., 2017; Gouel-Cheron et al., 2012; Wu et al., 2009; Kellum et al., 2007). Previous studies have demonstrated pyocyanin's ability to increase IL-6 in airway epithelial or urothelial cells (Rada et al., 2011; McDermott et al., 2013). By increasing pro-inflammatory concentrations of IL-6, pyocyanin may augment the acute phase reaction to *P. aeruginosa* infection. It is possible that reductions in plasma concentrations of IL-13, an anti-inflammatory cytokine produced by T helper 2 (Th2) cells that has been shown to inhibit secretion of IL-6, TNF-α and other inflammatory cytokines, contribute to an overzealous inflammatory response to pyocyanin (Zlotnik and Moore, 1991; Muchamuel et al., 1997; Baumhofer et al., 1998; Nicoletti et al., 1997). Conversely, IL-13 has been shown to play a protective role in cecal ligation and puncture (CLP) models of sepsis (Matsukawa et al., 2000), and reductions in IL-13 have been associated with increases in the neutrophil recruiter CXCL1 (Matsukawa et al., 2000), which was also modestly elevated in the plasma of pyocyanin-treated mice. Therefore, by blocking the protective anti-inflammatory processes of IL-13, pyocyanin may contribute to the longevity of *P. aeruginosa* survival. These changes in plasma concentrations of factors involved in inflammation may contribute to pyocyanin's ability to regulate body weight. However, since adipose tissue expression of several inflammatory modulators was not altered by pyocyanin, the source of these systemic factors is unclear.

Though advances in anti-inflammatory strategies have increased survival through the acute phase of sepsis, a growing number of patients are progressing to chronic critical illness (Kaneki, 2017). Cachexia, with no known therapeutic strategies, is a complication of chronic survivors of sepsis (Kaneki, 2017). We quantified measures of whole-body metabolism in male mice exposed to pyocyanin to define mechanisms for the observed reductions in body weight and fat mass. Interestingly, while both injections of pyocyanin lowered RER, EE, activity, and food intake of male mice, reductions were more robust and sustained upon repeated exposure. A shift towards a lower RER indicates that fat is being utilized as the predominant fuel source of pyocyanin-treated male mice. Similarly, fat is the preferred fuel of septic patients (Samra et al., 1996). Increased fat utilization and oxidation is further supported by an observed increase in basal lipolysis of fat explants, which coupled with greater fat oxidation may contribute to a loss of fat mass in male pyocyanin-treated mice. Reductions in energy expenditure of male pyocyanin-treated mice may relate to the observed reductions in physical activity that coincided with reduced body temperature. While food intake declined acutely in response to pyocyanin, these effects were not sustained and thus did not appear to contribute to sustained reductions in body weight.

Since sex differences in sepsis incidence and survival have been reported previously (Rhee et al., 2017; Martin et al., 2003), we contrasted effects of chronic pyocyanin exposures on body weight and fat mass in male and female mice. While both male and female mice exhibited sustained weight loss in response to pyocyanin, female mice lost weight after the first pyocyanin exposure. An important finding of the present study was an ability of pyocyanin to activate expression of CYP1a1 as a marker of AhR activation in adipose tissue, but not in liver of both sexes. This result was surprising in light of a much larger expression level of AhR in liver compared to adipose tissue (Uhlen et al., 2015; Carver et al., 1994; The Human Protein Atlas, 2019). Moreover, induction of CYP1a1 in adipose tissue was maintained two weeks after the last exposure to pyocyanin, supporting sequestration of lipophilic pyocyanin in adipose tissue. Indeed, pyocyanin was detected in adipose tissue 24 h after the last dose in male mice. However, we were not able to detect pyocyanin in adipose tissue of male or female mice at 2 weeks after the last dose. In addition to differences in the timing and degree of weight loss between males and females, results from this study suggest sex differences in the mechanisms of action of pyocyanin on adipose tissue biology. For example, adipose explants from males, but not females, exhibited increased basal lipolysis, while adipocytes differentiated from stem cells of pyocyanin-treated females had increased expression of TNF-α and AhR. Notably, changes in expression of these markers of inflammation and AhR activation in differentiated adipocytes occurred three weeks following the last exposure of female mice to pyocyanin. Therefore, pyocyanin's mechanism of weight loss and fat wasting appears to result from increased lipolysis in males and programmed changes in adipocyte stem cells in females. Other differences between sexes included levels of pro- or anti-inflammatory cytokines and/or markers of immune cell activation in plasma of male *versus* female pyocyanin-treated mice. The sexually dimorphic effects of pyocyanin may be due, in part, to sex differences in AhR responsiveness (Lee et al., 2015; Prokopec et al., 2015; Nault et al., 2017). Murine

studies have previously reported sex differences in the response to TCDD, including toxicity, CYP1a1 induction, wasting, and timing of peak response, that are partially explained by sex hormones (Prokopec et al., 2015; Pohjanvirta et al., 1993, 2012). Regardless, our results suggest that in both sexes, acute and chronic changes in plasma concentrations of inflammatory mediators may contribute to poor outcomes associated with chronic sepsis from *P. aeruginosa* by inhibiting the resolving phase of inflammation to allow for a more persistent infection.

In conclusion, results from this study demonstrate that pyocyanin reduced the differentiation of adipocytes *in vitro* and decreased body weight and fat mass when administered to male and female mice *in vivo*. Effects of pyocyanin to decrease body weight and fat mass were sustained for several weeks after the last exposure and appeared to involve different mechanisms in male *versus* female mice. These results indicate a potential role of pyocyanin in adipose wasting and cachexia associated with sepsis from *P. aeruginosa*. Future studies should elucidate the role of AhR in pyocyanin's sexual dimorphic effects on adipose cachexia in sepsis. Understanding pyocyanin's mechanisms of action could lead to novel therapeutic targets for septic cachexia produced by *P. aeruginosa*.

Grants, sponsors, and funding

Research reported was supported by grant P42ES007380 (LAC, AM, AS) from the National Institute of Environmental Health Sciences (NIEHS) within the National Institutes of Health (NIH). We also acknowledge NIH T32DK007778 for trainee support (NL). Indirect calorimetry and body lean and fat mass were quantified through research support cores within NIH P30 GM127211 (LAC).

Appendix A. Supplementary data

Supplementary data to this article can be found online at https://doi.org/10.1016/j.fct.2019.05.012.

Transparency document

Transparency document related to this article can be found online at https://doi.org/10.1016/j.fct.2019.05.012

References

Alexander, D.L., et al., 1998. Aryl-hydrocarbon receptor is an inhibitory regulator of lipid synthesis and of commitment to adipogenesis. J. Cell Sci. 111 (Pt 22), 3311–3322.
Argiles, J.M., et al., 2010. Consensus on cachexia definitions. J. Am. Med. Dir. Assoc. 11 (4), 229–230.
Arora, D., et al., 2018. Pyocyanin induces systemic oxidative stress, inflammation and behavioral changes in vivo. Toxicol. Mech. Methods 28 (6), 410–414.
Arsenescu, V., et al., 2008. Polychlorinated biphenyl-77 induces adipocyte differentiation and proinflammatory adipokines and promotes obesity and atherosclerosis. Environ. Health Perspect. 116 (6), 761–768.
Baker, N.A., et al., 2015. Effects of adipocyte aryl hydrocarbon receptor deficiency on PCB-induced disruption of glucose homeostasis in lean and obese mice. Environ. Health Perspect. 123 (10), 944–950.
Batista Jr., M.L., et al., 2013. Adipose tissue-derived factors as potential biomarkers in cachectic cancer patients. Cytokine 61 (2), 532–539.
Baumhofer, J.M., et al., 1998. Gene transfer with IL-4 and IL-13 improves survival in lethal endotoxemia in the mouse and ameliorates peritoneal macrophages immune competence. Eur. J. Immunol. 28 (2), 610–615.
Caldwell, C.C., et al., 2009. Pseudomonas aeruginosa exotoxin pyocyanin causes cystic fibrosis airway pathogenesis. Am. J. Pathol. 175 (6), 2473–2488.
Callahan, L.A., Supinski, G.S., 2009. Sepsis-induced myopathy. Crit. Care Med. 37 (10 Suppl. l), S354–S367.
Carver, L.A., Hogenesch, J.B., Bradfield, C.A., 1994. Tissue specific expression of the rat Ah-receptor and ARNT mRNAs. Nucleic Acids Res. 22 (15), 3038–3044.
Cavaillon, J.M., et al., 2003. Cytokine cascade in sepsis. Scand. J. Infect. Dis. 35 (9), 535–544.
Chousterman, B.G., Swirski, F.K., Weber, G.F., 2017. Cytokine storm and sepsis disease pathogenesis. Semin. Immunopathol. 39 (5), 517–528.
Crowell, K.T., Soybel, D.I., Lang, C.H., 2017. Inability to replete white adipose tissue during recovery phase of sepsis is associated with increased autophagy, apoptosis, and proteasome activity. Am. J. Physiol. Regul. Integr. Comp. Physiol. 312 (3), R388–R399.
Cruickshank, C.N., Lowbury, E.J., 1953. The effect of pyocyanin on human skin cells and leucocytes. Br. J. Exp. Pathol. 34 (6), 583–587.
Evans, W.J., et al., 2008. Cachexia: a new definition. Clin. Nutr. 27 (6), 793–799.
Fleischmann, C., et al., 2016. Assessment of global incidence and mortality of hospital-treated sepsis. Current estimates and limitations. Am. J. Respir. Crit. Care Med. 193 (3), 259–272.
Franco, F.O., et al., 2017. Cancer cachexia differentially regulates visceral adipose tissue turnover. J. Endocrinol. 232 (3), 493–500.
Fujii-Kuriyama, Y., Mimura, J., 2005. Molecular mechanisms of AhR functions in the regulation of cytochrome P450 genes. Biochem. Biophys. Res. Commun. 338 (1), 311–317.
Gouel-Cheron, A., et al., 2012. Early interleukin-6 and slope of monocyte human leukocyte antigen-DR: a powerful association to predict the development of sepsis after major trauma. PLoS One 7 (3), e33095.
Hall, S., et al., 2016. Cellular effects of pyocyanin, a secreted virulence factor of Pseudomonas aeruginosa. Toxins 8 (8).
Hotchkiss, R.S., Monneret, G., Payen, D., 2013. Sepsis-induced immunosuppression: from cellular dysfunctions to immunotherapy. Nat. Rev. Immunol. 13 (12), 862–874.
Jackson, E., et al., 2017. Adipose tissue as a site of toxin accumulation. Comp. Physiol. 7 (4), 1085–1135.
Jayaseelan, S., Ramaswamy, D., Dharmaraj, S., 2014. Pyocyanin: production, applications, challenges and new insights. World J. Microbiol. Biotechnol. 30 (4), 1159–1168.
Kaneki, M., 2017. Metabolic inflammatory complex in sepsis: septic cachexia as a novel potential therapeutic target. Shock 48 (6), 600–609.
Kellum, J.A., et al., 2007. Understanding the inflammatory cytokine response in pneumonia and sepsis: results of the genetic and inflammatory markers of sepsis (GenIMS) study. Arch. Intern. Med. 167 (15), 1655–1663.
La Merrill, M., et al., 2013. Toxicological function of adipose tissue: focus on persistent organic pollutants. Environ. Health Perspect. 121 (2), 162–169.
Lee, J., et al., 2015. Male and female mice show significant differences in hepatic transcriptomic response to 2,3,7,8-tetrachlorodibenzo-p-dioxin. BMC Genomics 16, 625.
Marques, M., et al., 2013. Critical illness induces nutrient-independent adipogenesis and accumulation of alternatively activated tissue macrophages. Crit. Care 17 (5), R193.
Martin, G.S., et al., 2003. The epidemiology of sepsis in the United States from 1979 through 2000. N. Engl. J. Med. 348 (16), 1546–1554.
Matsukawa, A., et al., 2000. Expression and contribution of endogenous IL-13 in an experimental model of sepsis. J. Immunol. 164 (5), 2738–2744.
McDermott, C., et al., 2013. Alterations in acetylcholine, PGE2 and IL6 release from urothelial cells following treatment with pyocyanin and lipopolysaccharide. Toxicol. Vitro 27 (6), 1693–1698.
Minasyan, H., 2017. Sepsis and septic shock: pathogenesis and treatment perspectives. J. Crit. Care 40, 229–242.
Moseti, D., Regassa, A., Kim, W.K., 2016. Molecular regulation of adipogenesis and potential anti-adipogenic bioactive molecules. Int. J. Mol. Sci. 17 (1).
Moura-Alves, P., et al., 2014. AhR sensing of bacterial pigments regulates antibacterial defence. Nature 512 (7515), 387–392.
Muchamuel, T., et al., 1997. IL-13 protects mice from lipopolysaccharide-induced lethal endotoxemia: correlation with down-modulation of TNF-alpha, IFN-gamma, and IL-12 production. J. Immunol. 158 (6), 2898–2903.
Nault, R., et al., 2017. Loss of liver-specific and sexually dimorphic gene expression by aryl hydrocarbon receptor activation in C57BL/6 mice. PLoS One 12 (9), e0184842.
Neves, R.X., et al., 2016. White adipose tissue cells and the progression of cachexia: inflammatory pathways. J Cachexia Sarcopenia Muscle 7 (2), 193–203.
Nicoletti, F., et al., 1997. Prevention of endotoxin-induced lethality in neonatal mice by interleukin-13. Eur. J. Immunol. 27 (6), 1580–1583.
Phillips, M., et al., 1995. Inhibition of 3T3-L1 adipose differentiation by 2,3,7,8-tetrachlorodibenzo-p-dioxin. J. Cell Sci. 108 (Pt 1), 395–402.
Pohjanvirta, R., Unkila, M., Tuomisto, J., 1993. Comparative acute lethality of 2,3,7,8-tetrachlorodibenzo-p-dioxin (TCDD), 1,2,3,7,8-pentachlorodibenzo-p-dioxin and 1,2,3,4,7,8-hexachlorodibenzo-p-dioxin in the most TCDD-susceptible and the most TCDD-resistant rat strain. Pharmacol. Toxicol. 73 (1), 52–56.
Pohjanvirta, R., et al., 2012. Unexpected gender difference in sensitivity to the acute toxicity of dioxin in mice. Toxicol. Appl. Pharmacol. 262 (2), 167–176.
Prokopec, S.D., et al., 2015. Sex-related differences in murine hepatic transcriptional and proteomic responses to TCDD. Toxicol. Appl. Pharmacol. 284 (2), 188–196.
Rada, B., et al., 2011. Reactive oxygen species mediate inflammatory cytokine release and EGFR-dependent mucin secretion in airway epithelial cells exposed to Pseudomonas pyocyanin. Mucosal Immunol. 4 (2), 158–171.
Remick, D.G., Xioa, H., 2006. Hypothermia and sepsis. Front. Biosci. 11, 1006–1013.
Rhee, C., et al., 2017. Incidence and trends of sepsis in US hospitals using clinical vs claims data, 2009-2014. J. Am. Med. Assoc. 318 (13), 1241–1249.
Rodbell, M., 1964. Metabolism of isolated fat cells. I. Effects of hormones on glucose metabolism and lipolysis. J. Biol. Chem. 239, 375–380.
Samra, J.S., Summers, L.K., Frayn, K.N., 1996. Sepsis and fat metabolism. Br. J. Surg. 83 (9), 1186–1196.
Schefold, J.C., Bierbrauer, J., Weber-Carstens, S., 2010. Intensive care unit-acquired weakness (ICUAW) and muscle wasting in critically ill patients with severe sepsis and septic shock. J Cachexia Sarcopenia Muscle 1 (2), 147–157.
Sharma, V.M., Puri, V., 2016. Mechanism of TNF-alpha-induced lipolysis in human adipocytes uncovered. Obesity 24 (5), 990.
Singer, M., et al., 2016. The third international consensus definitions for sepsis and septic shock (Sepsis-3). J. Am. Med. Assoc. 315 (8), 801–810.
Souza, S.C., et al., 2003. TNF-alpha induction of lipolysis is mediated through activation

of the extracellular signal related kinase pathway in 3T3-L1 adipocytes. J. Cell. Biochem. 89 (6), 1077–1086.
The Human Protein Atlas AhR [cited 2019 March 4]; Available from:: https://www.proteinatlas.org/ENSG00000106546-AHR/tissue.
Tsalik, E.L., et al., 2012. Discriminative value of inflammatory biomarkers for suspected sepsis. J. Emerg. Med. 43 (1), 97–106.
Uhlen, M., et al., 2015. Proteomics. Tissue-based map of the human proteome. Science 347 (6220), 1260419.
Wilson, R., et al., 1988. Measurement of Pseudomonas aeruginosa phenazine pigments in sputum and assessment of their contribution to sputum sol toxicity for respiratory epithelium. Infect. Immun. 56 (9), 2515–2517.
Wu, H.P., et al., 2009. Serial cytokine levels in patients with severe sepsis. Inflamm. Res. 58 (7), 385–393.
Zlotnik, A., Moore, K.W., 1991. Interleukin 10. Cytokine 3 (5), 366–371.